**Manuscript 4435 Revision 1**

# A comparison of the $Ca_3(PO_4)_2$ and $CaSiO_3$ systems, with a new structure refinement of tuite synthesized at 15 GPa and 1300 °C

**Richard M. Thompson[1*], Xiande Xie[2], Shuangmeng Zhai[3], Robert T. Downs[1], and Hexiong Yang[1]**

[1]Department of Geosciences, University of Arizona, Tucson, Arizona 85721-0077, USA

[2]Key Laboratory of Mineralogy and Metallogeny, Guangzhou Institute of Geochemistry, Chinese Academy of Sciences, Guangzhou 510640, China

[3]Key Laboratory of Orogenic Belts and Crustal Evolution, MOE; School of Earth and Space Sciences, Peking University, Beijing 100871, China

*Corresponding author: rmthomps@email.arizona.edu

## Abstract

Tuite, the high-pressure γ-form of the $Ca_3(PO_4)_2$ system, has been synthesized from chlorapatite at 15 GPa and 1300 °C using a multi-anvil apparatus and its crystal structure determined with single-crystal X-ray diffraction. It is isostructural with palmierite, with space group *R*-3*m* and unit-cell parameters $a = 5.2522(9)$ and $c = 18.690(3)$ Å. The structure of tuite is characterized by three distinct polyhedra, $PO_4$, $Ca1O_{12}$, and $Ca2O_{10}$, that are translationally interconnected in the sequence of $PO_4$-$Ca2O_{10}$-$Ca1O_{12}$-$Ca2O_{10}$-$PO_4$ along the *c* axis.

Comparison of the $CaSiO_3$ and $Ca_3(PO_4)_2$ polymorphic systems shows a striking resemblance in the evolution of atomic packing arrangements as the polymorphic density increases. In both cases, the Ca atoms are progressively incorporated into the (Ca + O) close-packed monolayers, consistent with the hypothesis that close-packing is a consequence of volume decrease as density increases. Based on this observation, we predict a possible high-pressure post-tuite phase.

**Keywords: tuite, $Ca_3(PO_4)_2$, whitlockite, close-packing, pseudowollastonite, wollastonite, perovskite, $CaSiO_3$**

## Introduction

There are four polymorphs in the $Ca_3(PO_4)_2$ system, denoted as α'-, α-, β-, and γ-phases. Among them, the α'-, α-, and β-phases are stable in the different temperature ranges, from 1470 to 1756, 1120 to1470, and room temperature to 1120 °C, respectively (Nurse et al. 1959; Fix et al. 1969; Famery et al. 1994; Knowles et al. 1999; Yashima and Sakai 2003), whereas the γ-phase, also known as tuite, is a high-pressure form and stable at least in the upper mantle conditions (Murayama et al. 1986; Xie et al. 2003). The $Ca_3(PO_4)_2$ system has been a subject of numerous investigations because α- and β-phases are important bioceramic materials in surgery and dentistry (e.g., Famery et al. 1994 and references therein) and tuite is a potential host for rare-earth elements (REE) and large lithophile elements (LLE) under the Earth's mantle conditions (Murayama et al. 1986; Sugiyama and Tokonami 1987; Xie et al. 2003; Zhai et al. 2010; 2011).

Tuite was first synthesized by Roux et al. (1978) from β-$Ca_3(PO_4)_2$ at 4 GPa and 950 °C and subsequently by Murayama et al. (1986) through compression of hydroxylapatite $Ca_5(PO_4)_3OH$ and fluorapatite $Ca_5(PO_4)_3F$ at 12-15 GPa and 1100-2300 °C. Its crystal structure was determined by Sugiyama and Tokonami (1987) using the sample made from hydroxylapatite at 12 GPa and 2300 °C. Recently, Zhai et al. (2009, 2010, 2011) have also obtained tuite through conversion of β-$Ca_3(PO_4)_2$ at 7 GPa and 1200 °C to measure its high-pressure and high-temperature properties with Raman spectroscopy and powder X-ray diffraction. Natural tuite was originally described by Chen et al. (1995) as a high-pressure polymorph of chlorapatite,

$Ca_5(PO_4)_3Cl$, in shock-induced melt veins of the Sixiangkou L6 chondrite, which contains 3.72 wt.% Cl, as compared to 4.84 wt.% Cl in chlorapatite. Xie et al. (2002, 2003) reported the finding of tuite that is believed to have transformed from whitlockite in the shocked veins of the Suizhou L6 chondrite. Their Raman spectra of tuite, however, do not match those given by Chen et al. (1995). The recent study (Xie et al., submitted) has demonstrated that the Raman spectra obtained by Chen et al. (1995) are actually a combination (or mixture?) of tuite and chlorapatite, presumably stemming from the incomplete transformation from chlorapatite to tuite. Xie and Chen (2008) discussed the plausible conditions for the tuite formation from whitlockite and chlorapatite. Nonetheless, it remains unclear whether tuite transformed from chlorapatite can contain a significant amount of Cl. This study reports the first synthesis of tuite from chlorapatite at high pressure and temperature and its structure refinement with single-crystal X-ray diffraction. Moreover, by comparing the $Ca_3(PO_4)_2$ system with the $CaSiO_3$ system in terms of close-packing schemes, we present a new perspective in understanding the tuite structure and predict a possible high-pressure post-tuite phase.

Identifying the packing schemes of the anion arrangements of crystal structures is one of the fundamental tasks for a comprehensive understanding of mineral systematics. Interest in the packing of spherical atoms as the basis of matter goes back at least to the late $16^{th}$ century (Hales 2000). Many ionic crystal structures have been successfully rationalized as composed of close-packed (CP) arrangements of large anions with small cations filling the interstitial voids in the anion scaffold. An example of a useful application of this concept is Pauling's (1929) radius-ratio rule for predicting cation coordination numbers from cation : anion radius ratios. Underlying the concept of large anions/small cations is the assumption that oxygen anions form CP arrangements to minimize structural volume. From this perspective, there is nothing to bar

cations from inclusion with O atoms in CP arrangements should size considerations allow. This is in fact seen in the perovskite structure (c.f. Klein and Dutrow 2008).

The fundamental building blocks of three dimensional closest-packed arrangements are two dimensional CP monolayers, in which each sphere is in contact with six nearest neighbors. The CP stacking of monolayers give rise to interstitial (cation) sites that are trigonal planar, tetrahedral, or octahedral. All tetrahedral sites in any CP arrangement have bases perpendicular to a stacking direction with apices pointing parallel to the stacking vectors, and therefore have at least one face parallel to at least one face in all other tetrahedra. Any two tetrahedra sharing corners have either coplanar bases containing the shared sphere or parallel bases with a shared apical sphere, forming a unit resembling an hourglass. Crystal structures that violate these conditions are either very distorted or not based on the close-packing arrangement. Nevertheless, small systematic alterations to CP monolayers can create layers that can be stacked forming tetrahedral and high-coordination number sites that violate these rules (Thompson et al. 2012).

CP monolayers are typically distinctive but may be difficult to recognize in minerals that are quite distorted from closest-packed. Thompson and Downs (2001) introduced a parameter, $U_{cp}$, to quantify the degree of distortion of the oxygen anion skeletons of minerals from the perfectly closest-packed arrangement. In the cubic closest-packing or CCP (hexagonal closest-packing or HCP) case, $U_{cp}$ is the minimum mean square displacement of 675 (677) corresponding anions contained in a spherical volume of space in the observed and ideal structures. This parameter is calculated by allowing the ideal structure to translate, rotate, and isotropically expand or compress relative to the observed structure until the minimum value ($U_{cp}$) is found. A value of zero for $U_{cp}$ indicates an anion skeleton that is perfectly closest-packed, with distortion increasing as $U_{cp}$ gets larger. A value of 1 indicates an oxygen arrangement that is

105 extremely distorted. We will use $U_{cp}$ in this paper to examine the distortion from perfect closest-
106 packing of minerals of interest. In addition, we will adopt the terms eutaxy and eutactic
107 arrangement to describe an arrangement with the same spatial relationships as close-packing, but
108 where the packed units are not necessarily believed to be in contact (after O'Keeffe and Hyde
109 1996), i.e. as a more general term that can be used synonymously.
110

111 **Experimental**

112 The tuite sample used in this study was synthesized using synthetic chlorapatite as
113 starting material at high pressure and high-temperature. First, reagent-grade $CaCO_3$, $NH_4Cl$ and
114 $NH_4H_2PO_4$ powders were mixed in a proportion corresponding to the $Ca_5(PO_4)_3Cl$ stoichiometry.
115 The mixture was ground for 2 hours in an agate mortar and pressed into pellets with a diameter
116 of 5 mm under uniaxial pressure of 30 MPa. The pellets were then sintered in a conventional
117 muffle furnace at 1000 °C for 36 hours to form a single phase of $Ca_5(PO_4)_3Cl$, which was
118 confirmed by powder X-ray diffraction. The $Ca_5(PO_4)_3Cl$ powder was then put into a Pt capsule
119 to synthesize tuite at 15 GPa and 1300 °C for 24 hours using a multi-anvil apparatus. The high-
120 pressure and high-temperature experimental details were described by Xue et al. (2009). The
121 final product was characterized by microfocused X-ray diffraction and Raman spectroscopy.
122 Chemical compositions of the synthesized sample were determined by an electron probe
123 microanalyzer (JXA-8800) operated at 15 kV and 12 nA. The average composition (10 analysis
124 points) is (wt.%) CaO 54.2(3), $P_2O_5$ 46.2(7), and total =100.4(9), yielding an empirical formula
125 (based on 8 O *apfu*) $Ca_{2.98}(P_{1.01}O_4)_2$.

126 Single-crystal X-ray diffraction data of tuite were collected from a nearly equi-
127 dimensional crystal (0.04 x 0.05 x 0.05 mm) with frame widths of 0.5° in ω and 30 s counting

time per frame. All reflections were indexed on the basis of a trigonal unit-cell (Table 1). The intensity data were corrected for X-ray absorption using the Bruker program SADABS. The systematic absences of reflections suggest possible space groups *R*32*,* *R*3*m,* or *R*-3*m*. The crystal structure was solved and refined using SHELX97 (Sheldrick 2008) based on the space group *R*-3*m*, because it yielded the best refinement statistics in terms of bond lengths and angles, atomic displacement parameters, and *R* factors. The positions of all atoms were refined with anisotropic displacement parameters. During the structure refinements, the ideal chemistry was assumed. Final coordinates and displacement parameters of atoms in tuite are listed in Table 2, and selected bond-distances in Table 3.

## Discussion

### *The structure of tuite*

Tuite belongs to a vast group of compounds with the palmierite-type structure and the general chemical formula $M_3(XO_4)_2$, where M = Ba, Sr, Ca, Pb, Rb, K, Na, $NH_4$, Tl, REE and X = V, Cr, P, S, As. Depending on the chemistry, the palmierite-type materials can exhibit various interesting optical, transport, catalytic, dielectric, and ferroelectric properties (e.g., Leonidova and Leonidova 2008; Sahoo et al. 2010 and references therein). The X cation in the palmierite-type structure is tetrahedrally coordinated, whereas the M cations occupy two symmetrically nonequivalent sites, M1 and M2. The M1 site displays a (6 + 6) coordination, with six M1-O bond lengths markedly shorter than the other six M1-O bonds. In contrast, the M2 site is ten-coordinated. Specifically for tuite, our structure data are very comparable with those determined by Sugiyama and Tokonami (1987) (Tables 1 and 3). The $PO_4$ tetrahedron is slightly distorted, with three P-O2 bond distances (1.542 Å) longer than the one P-O1 bond distance (1.521 Å). The

average M1-O and M2-O bond distances are 3.0377 and 2.4404 Å, respectively. The detailed linkage among the $PO_4$, $M1O_{12}$, and $M2O_{10}$ polyhedra has been elucidated by Sugiyama and Tokonami (1987). In the following, we will offer a different view of the tuite structure by placing it into the context of the $Ca_3(PO_4)_2$ and $CaSiO_3$ polymorphic systems. Both systems contain at least four phases, in each case with Ca as the only non-tetrahedral cation; both contain phases (β-$Ca_3(PO_4)_2$ and pseudowollastonite) that exhibit large, multi-polyhedral structural subunits functioning as ligands, and both contain structures that incorporate Ca cations and O anions into a single packing arrangement. To better understand the $Ca_3(PO_4)_2$ system, we will first review the $CaSiO_3$ system and use the principles that apparently govern both of them to make a prediction.

***Review of the $CaSiO_3$ system***

There are four polymorphs in the $CaSiO_3$ system: pseudowollastonite (Yang and Prewitt 1999), wollastonite (Ohashi and Finger 1978), a high-pressure phase (Trojer 1969), and Ca-perovskite (Caracas and Wentzcovitch 2006), with densities of 2.90, 2.95, 3.05, and 4.33 g/cm$^3$, respectively (Table 4).

Pseudowollastonite is composed of layers of ternary $Si_3O_9$ rings (Figure 1a) alternating with layers of 8-coordinated Ca-polyhedra stacked along **c***. The ternary rings themselves are in two-dimensional eutactic arrangement, and the layers of rings can be thought of as functioning as close-packed monolayers of $[Si_3O_9]^{6-}$ ligands. These ligands are not in three-dimensional eutaxy, and there are four different monolayer positions (ABCD) instead of the three (ABC) of close-packed arrangements (Figure 1b).

However, the entire structure of pseudowollastonite can also be regarded as based on close-packing of O and Ca atoms, with each organized into well-defined layers stacked along **c*** in the sequence ABABACACABABACAC (Figure 2). Three quarters of these layers, including the Ca layers, are easily recognizable as close-packed monolayers. As an example, Figure 3 illustrates in isolation the four Ca monolayers labeled A in Figure 2, viewed down the stacking direction, **c***, with all other atoms removed. Clearly, the atoms in these four layers align and are equivalent in terms of their function in the stacking sequence. The remaining layers labeled A contain O atoms coplanar with Si atoms in six-membered atomic rings (Figure 4a, again viewed down the stacking vector). These layers may at first appear to be non-CP, but Figure 4b shows the correspondence between the O atoms in these layers and the Ca atoms in the nearest Ca-monolayer (labeled A). Thus, these O-layers are actually equivalent to A layers, but distorted by the presence of the coplanar Si atoms. This distortion allows for the formation of tetrahedral sites with geometrical relationships that would not be possible in the perfectly closest-packed arrangement of spheres with stacking sequence ABABACAC.

Consideration of just the O atoms in pseudowollastonite also yields a CP arrangement with stacking sequence BABCAC, or, equivalently, ABACBC. When every octahedral site formed by two O-monolayers is occupied (brucite-type layer), the cations form a eutactic monolayer of their own. This begs the question: should the Ca-monolayers be considered part of the packing, or just cations in the interstitial sites of a CP oxygen skeleton? In any ideal CP arrangement, the distance between monolayers is twice the distance between the cation layer and the nearest monolayer. In pseudowollastonite, the average distance between O-monolayers is only 38% longer than the average distance between Ca- and O-monolayers. This is consistent with the Ca atoms functioning as part of the packing arrangement, albeit with an effective radius

196 approximately 70% of that of the O atoms. Electron density analysis of pseudowollastonite
197 could provide sizes for its ionic radii.

198 Wollastonite is a member of the pyroxenoid group of minerals, often described as similar
199 to the pyroxene group because both groups contain single tetrahedral silicate chains connecting
200 layers of chains of octahedrally coordinated cations (c.f. Klein and Dutrow 2008). Figure 5a
201 shows the wollastonite tetrahedral chain and its relationship to the octahedral chain with which it
202 shares its apical O atoms. Figure 5b illustrates the analogous structural subunits in hypothetical
203 ideal CCP and HCP wollastonite chains, formed from the two possible CP arrangements of three
204 CP monolayers, demonstrating that the wollastonite tetrahedral chain does not directly
205 correspond to a CP arrangement. In fact, it can best be described as a hybrid between the
206 possible CCP and HCP configurations. Therefore, wollastonite is very distorted from either CCP
207 or HCP, and our software failed to calculate a $U_{cp}$ value for it, with or without including Ca in
208 the packing scheme.

209 Trojer (1969) presented a refinement of a $CaSiO_3$ phase synthesized at 6.5 GPa and 1300
210 °C. Our program calculated a $U_{cp}$ value of 2.6 $Å^2$ from ideal CCP for the oxygen anion
211 arrangement, but failed when any Ca was included in the packing arrangement. This value
212 indicates an extremely distorted structure, and it is difficult to recognize distinct CP layers in the
213 structure. Figure 6a illustrates the crystal structure viewed down zone [2-1-1], not identified as a
214 CP stacking direction by our software. It is composed of non-eutactic Ca layers alternating with
215 layers containing both O and Ca, one Ca layer for every two (O + Ca) layers. Figure 6b displays
216 an (O + Ca) layer viewed down zone [425] (face pole (111)), showing Ca incorporated into the O
217 layers, in which each Ca atom is surrounded by five nearest O atoms. The Ca : O ratio in each
218 (Ca + O) layer, nevertheless, is 1: 9. Applying a two-dimensional radius ratio analysis to this

219 configuration yields a Ca radius 70% that of oxygen, the same value derived through analysis of
220 the stacking sequence of pseudowollastonite.

221 $CaSiO_3$ assumes the perovskite structure at extremely high pressure (hereafter referred to
222 as Ca-pv). Using density functional theory, Caracas and Wentzcovitch (2006) calculated
223 hypothetical room-condition cell parameters for ideal cubic Ca-pv (positional parameters are
224 fixed). This structure has a $U_{cp}$ value of 0, meaning that it is perfectly closest-packed, with all Ca
225 atoms incorporated into the CP monolayers in a Ca : O ratio of 1 : 3 (Fig. 7).

226 In short, as the $CaSiO_3$ polymorphs increase in density, Ca is progressively incorporated
227 into the layers of O atoms. In pseudowollastonite, the lowest density polymorph examined here,
228 Ca is excluded from the O monolayers, forming monolayers of its own. In wollastonite, the Ca
229 atoms occupy classic interstitial octahedral sites. In the higher density synthetic phase of Trojer
230 (1969), one-third of the Ca atoms are incorporated into layers with O atoms. Finally, in the
231 perovskite structure, all Ca atoms combine with O atoms to form (Ca + O) CP monolayers.
232
233 ***The $Ca_3(PO_4)_2$ system***

234 This set of polymorphs includes α-$Ca_3(PO_4)_2$ (Mathew et al. 1977), β-$Ca_3(PO_4)_2$ (Dickens
235 et al. 1974), and tuite or γ-$Ca_3(PO_4)_2$ (this work), with densities 2.81, 3.07, and 3.46 g/cm$^3$,
236 respectively (Table 4). Note that the α'-phase is excluded from the discussion here, because it is
237 an unquenchable high-temperature form and its structure symmetry is still a matter of
238 disputation. For example, by means of high-temperature neutron powder diffraction, Knowles et
239 al. (1999) and Yashima and Sakai (2003) obtained space group $P6_3/mmc$ (at 1525 °C) and $P\text{-}3m$
240 (at 1508 °C), respectively.

241 The structure of α-$Ca_3(PO_4)_2$ consists of 12 nonequivalent isolated $PO_4$ tetrahedra sharing
242 corners and edges with 18 nonequivalent Ca-polyhedra of various coordination numbers and
243 geometries. We were unable to calculate a $U_{cp}$ value for this structure, nor identify any distinct
244 atomic layers.

245 β-$Ca_3(PO_4)_2$ possesses the whitlockite-type structure. Like pseudowollastonite, it is also
246 based on an eutactic arrangement of large ligands, but, unlike pseudowollastonite, we uncovered
247 no packing arrangement involving individual atoms. Some indistinct atomic layering is evident
248 when viewing the structure perpendicular to **c**, including non-CP layers that are distorted in three
249 dimensions but incorporate Ca in a Ca : O ratio of 5 : 6. The β-phase appears to be intermediate
250 between α-$Ca_3(PO_4)_2$, with its complete absence of layering, and tuite, which has a very distinct
251 layered structure (as described below).

252 The large β-phase ligands are in three-dimensional distorted eutaxy and have a formula
253 $[Ca(PO_4)_6]^{16-}$ (Figure 8a). They consist of central Ca octahedra sharing corners with six $PO_4$
254 tetrahedra, thus forming flattened disks (or "pinwheels", see Moore 1973) that stack in a
255 distorted CCP arrangement. The ligands' central Ca atoms have ideal CCP positional parameters,
256 but their flattened geometry creates a very distorted cell, leading to an enormous $U_{cp}$ value of
257 24.7Å$^2$. As in pseudowollastonite, the ligands cannot be considered to be in contact, as they are
258 separated by $Ca^{2+}$ cations. For an in-depth discussion of the whitlockite-type structure, see Tait
259 et al. (2011).

260 Tuite bears a superficial visual resemblance to β-$Ca_3(PO_4)_2$ because one can visualize
261 "pinwheels" (Moore 1973) in both structures (Figure 8b). However, the pinwheels in tuite are
262 combined into corner-sharing polymerized polyhedral layers, not containing distinct pinwheel
263 ligands. As discussed below, Ca in tuite is part of the packing arrangement, and the Ca2-O2

bonds bind the polyhedral layers together to form a three-dimensional structure. The Ca participation in the packing scheme increases density relative to the β-phase and allows a much more distinct layering of individual atoms. We analyze tuite from this perspective.

All Ca atoms in tuite are incorporated with oxygen into eutactic monolayers of individual atoms (as opposed to layers of polyhedra) and stacked in a non-CP sequence along **c** that can be described as A'ABA'CAA'BC (Figure 9). Figures 10a and b illustrate tuite's two types of (Ca + O) layers - A' and A (B and C are equivalent to A, and are stacked in eutactic relationship with A - but not A' - along **c**), respectively. Layers A, B, and C are perovskite-type layers (Figure 7), and form a distorted CCP arrangement of O and Ca atoms. Layer A' is also eutactic, but contains only three unit cell atoms for every four in layer A (a Ca : O ratio of 1 : 2 instead of 1 : 3 in the pv-type monolayers). This allows for an unusual geometric relationship with the A (and B and C) layers in which two-thirds of the A' atoms (all of the Ca and one-half of the O) are in eutactic relationship with A, but one-half of the O atoms are on vectors parallel to **c** that also pass through Ca atoms in layer A (these vectors are not illustrated in Figure 9 – lines shown are the unit cell). For example, in Figure 10a and b, there are atoms in both layers at [2/3, 1/3, z].

The non-eutactic packing arrangement of tuite increases its bulk Ca : O ratio from 3 : 9 in Ca-pv to 3 : 8. Given the similarities between the $Ca_3(PO_4)_2$ and the $CaSiO_3$ polymorphic systems, it is a reasonable prediction that tuite will transform under pressure to a structure that has a eutactic packing arrangement incorporating both the oxygen and calcium atoms. However, such a structure would be constrained to have the same number of atoms per unit cell in each monolayer, unlike tuite. While Ca : O ratios in different monolayers could vary, the bulk Ca : O ratio would still have to be 3 : 8. We have not discovered an arrangement that would meet these

286 constraints and distribute Ca as "evenly" in the monolayers as it is in the A' monolayers and in
287 the pv-type layers (i.e. every nearest neighbor Ca-Ca distance is the same in both layer types).
288
289 ***Possible OH- or F-bearing analogue of tuite***
290 A number of palmierite-type compounds are capable of incorporating H atoms into their
291 structures as an essential component, such as previously observed for $Cs_3H(SeO_4)_2$ (Merinov et
292 al. 1990; Sonntag et al. 1998), $Rb_3H(SeO_4)_2$ (Baranov et al. 1987; Magome et al. 2009),
293 $Tl_3H(SO_4)_2$ (Matsuo et al., 2002), $K_3H(SO_4)_2$ (Makarova et al. 2010). This, thus, calls it into
294 question whether tuite can accommodate any H atoms during its formation from hydroxylapatite
295 and whitlockite, ideally $Ca_9Mg(PO_4)_6(PO_3OH)$, at high temperatures and pressures. A possible
296 mechanism for introducing H to the tuite structure might be through the substitution ($Na^+ + H^+$
297 $\rightarrow Ca^{2+}$), giving rise to a chemical formula $Ca_2NaH(PO_4)_2$ or $CaNa_2(PO_3OH)_2$. Interestingly,
298 tuite from the Suizhou L6 chondrite is found to contain a significant amount of Na,
299 $(Ca_{2.51}Mg_{0.29})_{2.80}Na_{0.28}(P_{1.01}O_4)_2$ (Xie et al. 2003). Moreover, since tuite can also be obtained
300 from fluorapatite at high temperatures and pressures, and the whitlockite-bobdownsite (the F-
301 analogue of whitlockite) solid solution has been found in various meteorites (e.g., Treiman et al.
302 1994; Gleason et al. 1997; Lodders 1998; Zipfel et al. 2000; Folco et al. 2000; Wadhwa et al.
303 2001; Mikouchi et al. 2001; Gnos et al. 2002), one may also propose, by the same token, the
304 possible F-bearing analogue of tuite through the coupled substitution $Na^+ + F^- \rightarrow Ca^{2+} + O^{2-}$,
305 leading to the chemical formula $CaNa_2(PO_3F)_2$. Apparently, further high-temperature and high-
306 pressure experiments with appropriate chemical compositions could shed light on the above
307 proposals.
308

## Acknowledgements

We gratefully acknowledge the funding support from the National Natural Science Foundation of China (Grant No. 41172046 to X.X. and Grant No. 40973045 to S.Z.), and the Science Foundation Arizona. We are also indebted to Dr. Fabrizio Nestola and an anonymous reviewer for their valuable suggestions, which have improved the quality of our manuscript.

## References

Baranov, A.I., Makarova, I.P., Muradyan, L.A., Tregubchenko, A.V., Shuvalov, L.A., and Simonov, V.I. (1987) Phase transition and proton conductivity in $Rb_3H(SeO_4)_2$ crystals. Kristallografiya, 32, 400-407.

Caracas, R. and Wentzcovitch, R.M. (2006) Theoretical determination of the structures of the $CaSiO_3$ perovskites. Acta Crystallographica, B62, 1025-1030.

Chen, M., Wopenka, B., Xie, X., and El Goresy, A. (1995) A new high-pressure polymorph of chlorapatite in the shocked chondrite Sixiangkou (L6). Lunar Planetary Sciences, XXVI, 237-238.

Dickens, B., Schroeder, L.W., and Brown, W.E. (1974) Crystallographic studies of the role of Mg as a stabilizing impurity in β-$Ca_3(PO_4)_2$ I. The crystal structure of pure β-$Ca_3(PO_4)_2$. Journal of Solid State Chemistry, 10, 232-248.

Famery, R., Richard, N., and Boch, P. (1994) Prepartion of α- and β-tricalcium phosphate ceramics, with and without magnesium additions. Ceramics International, 20, 327-336.

Fix, W., Heymann, H., and Heinke, R. (1969) Subsolidus relations in the system $2CaO{\cdot}SiO_2$-$3CaO{\cdot}P_2O_5$. Journal of American Ceramic Society, 52, 346-347.

Folco, L., Franchi, I.A., D'Orazio, M., Rocchi, S., and Schultz, L. (2000) A new Martian

meteorite from the Sahara: the shergottite Dar al Gani 489. Meteoritics and Planetary Sciences, 35, 827-839.

Gleason, J.D., Kring, D.A., Hill, D.H., and Boynton, W.V. (1997) Petrography and bulk chemistry of Martian lherzolite LEW 88516. Geochimica et Cosmochimica Acta, 61, 4007-4014.

Gnos, E., Hofmann, B., Franchi, I.A., Al-Kathiri, A., Hauser, M., and Moser, L. (2002) Sayh al Uhaymir 094: a new Martian meteorite from the Oman desert. Meteoritics and Planetary Sciences, 37, 835-854.

Hales, T.C. (2000) Cannonballs and honeycombs. Notices of the American Mathematical Society, 47, 440-449.

Klein, C. and Dutrow, B. (2008) *The Manual of Mineral Science*. John Wiley & Sons, Hoboken, New Jersey.

Knowles, J.C., Gibson, I.R., and Abrahams, I. (1999) High temperature phase transitions in $Ca_3(PO_4)_2$ measured by neutron diffraction. Bioceramics, 12, 341-344.

Leonidova, O.N. and Leonidova, E.I. (2008) Synthesis and electrophysical properties of cation conductors $Sr_{3-3x}La_{2x}(V_{1-y}P_yO_4)_2$ with palmierite structure. Solid State Ionics, 179, 188-191.

Lodders, K. (1998) A survey of shergottite, nakhlite and chassigny meteorites whole-rock compositions. Meteoritics and Planetary Sciences, 33 (Suppl.), A183-A190.

Magome, E., Sawada, K., and Komukae, M. (2009) X-ray structure analysis of $Rb_3H(SeO_4)_2$ in the high-temperature phase. Ferroelectrics, 378, 157-162.

Makarova, I.P., Chernaya, T.S., Filaretov, A.A., Vasil'ev, A.L., Verin, I.A., Grebenev, V.V., and Dolbinina, V.V. (2010) Investigation of the structural conditionality for changes in physical properties of $K_3H(SO_4)_2$ crystals. Kristallografiya, 55, 429-439.

356 Mathew, M., Schroeder, L.W., Dickens, B., and Brown, W.E. (1977) The crystal structure of α-
357 $Ca_3(PO_4)_2$. Acta Crystallographica, B33, 1325-1333.
358 Matsuo, Y., Kawachi, S., Shimizu, Y., and Ikehata, S. (2002) Trithallium hydrogen bis(sulfate),
359 $Tl_3H(SO_4)_2$, in the super-ionic phase by X-ray powder diffraction. Acta Crystallographica,
360 C58, i92-i94.
361 Merinov, B.V., Baranov, A.I., and Shuvalov, L.A. (1990) Crystal structure and mechanism of
362 protonic conductivity of a superionic phase of $Cs_3H(SeO_4)_2$. Kristallografiya, 35, 355-360.
363 Mikouchi, T., Miyamoto, M., and McKay, G.A. (2001) Mineralogy and petrology of the Dar al
364 Gani 476 Martian meteorite: implications for its cooling history and relationship to other
365 shergottites. Meteoritics and Planetary Sciences, 36, 531-548.
366 Moore, P.B. (1973) Bracelets and pinwheels: A topological-geometrical approach to the calcium
367 orthosilicate and alkali sulfate structures, American Mineralogist, 58, 32-42.
368 Murayama, J.K., Nakai, S., Kato, M., and Kumazawa, M. (1986) A dense polymorph of
369 $Ca_3(PO_4)_2$: A high pressure phase of apatite decomposition and its geochemical significance.
370 The Physics of the Earth and Planetary Interiors, 44, 293–303.
371 Nurse, R.W., Welch, J.H., and Gutt, W. (1959) High-temperature phase equilibria in the system
372 dicalcium silicate-tricalcium phosphate. Journal of Chemical Society, 1959, 1077-1083.
373 Ohashi, Y. and Finger, L.W. (1978) The role of octahedral cations in pyroxenoid crystal
374 chemistry. I. Bustamite, wollastonite, and the pectolite-schizolite-serandite series. American
375 Mineralogist, 63, 274-288.
376 O'Keeffe, M. and Hyde, B.G. (1996) *Crystal Structures*. Mineralogical Society of America,
377 Washington, D.C.
378 Pauling, L. (1929) The principles determining the structure of complex ionic crystals. Journal of

the American Chemical Society, 51, 1010-1026.

Roux, P., Louër, D., and Bonel, G. (1978) Sur une novelle forme cristallite du phosphate tricalcique. Comptes Rendus Hebdomadaires Des Seances De L Academie Des Sciences Serie C, 286, 549–551.

Sahoo, P.P., Gaudin, E., Darriet, J., and Guru Row, T.N. (2010) Synthesis, characterization, and crystallographic study of the PbO-$Bi_2O_3$-$V_2O_5$ system: $Pb_{3-x}Bi_{2x/3}V_2O_8$ (0.20 < x 0.50). Inorganic Chemistry, 49, 5603-5610.

Sheldrick, G. M. (2008) A short history of *SHELX*. Acta Crystallographica, A64, 112-122.

Sonntag, R., Melzer, R., Knight, K.S., and Radaelli, P.G. (1998) Structural study of the proton conductor $Cs_3H(SeO_4)_2$ by high resolution neutron powder diffraction. Materials Science Forum, 278, 726-731.

Sugiyama, S., and Tokonami, M. (1987) Structure and crystal chemistry of a dense polymorph of tricalcium phosphate $Ca_3(PO_4)_2$: A host to accommodate large lithophile elements in the Earth's mantle. Physics and Chemistry of Minerals, 15, 125–130.

Tait, K.T., Barkley, M.C., Thompson, R.M., Origlieri, M., Evans, S.H., Prewitt, C.T., and Yang, H. (2011) Bobdownsite, a new member of the whitlockite-group from Big Fish River, Yukon, Canada. The Canadian Mineralogist, 49, 1065-1078.

Thompson, R.M., and Downs, R.T. (2001) Quantifying distortion from ideal closest-packing in a crystal structure with analysis and application. Acta Crystallographica, B57, 119-127.

Thompson, R.M., Yang, H., and Downs, R.T. (2012) Packing systematics and structural relationships of the new copper molybdate markascherite and related minerals. American Mineralogist, 97, 1977-1986.

Treiman, A.H., McKay, G.A., Bogard, D.D., Mittlefehld, D.W., Wang, M-S., Keller, L., Lipschutz, M.E., Lindstrom, M.M., and Garrison, D. (1994) Comparison of the LEW 88516

and ALHA77005 Martian meteorites: similar but distinct. Meteoritics, 29, 581-592.

Trojer, F.J. (1969) The crystal structure of a high-pressure polymorph of $CaSiO_3$. Zeitschrift für Kristallographie, 130, 185-206.

Wadhwa, M., Lentz, R.C.F., McSween Jr., H.Y., and Crozaz, G. (2001) A petrologic and trace element study of Dar al Gani 476 and Dar al Gani 489: twin meteorites with affinities to basaltic and lherzolitic shergottites. Meteoritics and Planetary Sciences, 36, 195-208.

Xie, X. and Chen, M. (2008) Formation conditions of tuite. Geochimica, 37, 297-303 (in Chinese with English abstract).

Xie, X., Minitti, M.E., Chen, M., Mao, H.K., Wang, D., Shu, J., and Fei, Y. (2002) Natural high-pressure polymorph of merrillite in the shock vein of the Suizhou meteorite. Geochimica et Cosmochimica Acta, 66, 2439-2444.

Xie, X., Minitti, M.E., Chen, M., Mao, H.K., Wang, D., Shu, J., Fei, Y. (2003) Tuite, γ-$Ca_3(PO_4)_2$ : a new mineral from the Suizhou L6 chondrite. European Journal of Mineralogy, 15, 1001-1005.

Xie, X., Zhai, S., Chen, M., and Yang, H. (submitted) Tuite, γ-$Ca_3(PO_4)_2$, formed from chlorapatite decomposition in the shock vein of the Suizhou L6 chondrite. Meteoritics & Planetary Sciences.

Xue, X., Zhai, S., and Kanzaki, M. (2009) Si-Al distribution in high-pressure $CaAl_4Si_2O_{11}$: A $^{29}Si$ and $^{27}Al$ NMR study. American Mineralogist, 94, 1739-1742.

Yang, H. and Prewitt, C.T. (1999) On the crystal structure of pseudowollastonite ($CaSiO_3$). American Mineralogist, 84, 929-932.

Yashima, M. and Sakai, A. (2003) High-temperature neutron powder diffraction study of the structural phase transition between a and a' phases in tricalcium phosphate $Ca_3(PO_4)_2$.

426 Chemical Physics Letters, 372, 779-783.
427 Zhai, S., Liu, X., Shieh, S. R., Zhang, L., and Ito, E. (2009) Equation of state of γ-tricalcium
428 phosphate, γ-$Ca_3(PO_4)_2$, to lower mantle pressures. American Mineralogist, 94, 1388-1391.
429 Zhai, S., Wu, X., and Ito, E. (2010) High-pressure Raman spectra of tuite, γ-$Ca_3(PO_4)_2$. Journal
430 of Raman Spectroscopy, 41, 1011-1013.
431 Zhai, S., Xue, W., Lin, C., and Wu, X. (2011) Raman spectra and X-ray diffraction of tuite at
432 various temperatures. Physics and Chemistry of Minerals, 38, 639-646.
433 Zipfel, J., Scherer, P., Spettel, B., Dreibus, G. and Schultz, L. (2000) Petrology and chemistry of
434 the new shergottite Dar al Gani 476. Meteoritics and Planetary Sciences, 35, 95-106.
435

436 **List of Figure Captions**

437 Figure 1a. A layer of $[Si_3O_9]^{6-}$ ligands in the psuedowollastonite structure.

438 Figure 1b. The geometric relationship among layers of $[Si_3O_9]^{6-}$ ligands looking down **c***.

439 Figure 2. The atomic packing arrangement of pseudowollastonite, illustrating the incorporation
440 of Ca atoms into the arrangement.

441 Figure 3. The eutactic Ca monolayers that intersect the unit cell in psuedowollastonite viewed in
442 isolation down the stacking direction, **c***, with all other atoms removed. This cartoon shows
443 that these layers all align and are all A layers.

444 Figure 4a. (O + Si) layers viewed down **c*** in psuedowollastonite.

445 Figure 4b. The relationship between the oxygen atoms in the (O + Si) layers in
446 psuedowollastonite and the nearest Ca layer along **c***, illustrating that the O layers are
447 distorted A layers in the stacking sequence.

448 Figure 5a. The tetrahedral and octahedral chains in wollastonite (Ohashi and Finger 1978).

449 Figure 5b. Hypothetical ideal CP wollastonite analogs.

450 Figure 6a. Layering in the high-pressure synthetic $CaSiO_3$ phase of Trojer (1969) looking down
451 zone [2-1-1].

452 Fibure 6b. The (O + Ca) layer viewed down zone [425] showing the incorporation of Ca into O
453 layers in the high-pressure $CaSiO_3$ phase of Trojer (1969).

454 Figure 7. The perfectly closest-packed monolayer of O anions and Ca cations, viewed along
455 [111], in a hypothetical room condition perovskite (Caracas and Wentzcovitch 2006).

456 Figure 8a. A layer of "pinwheels" viewed down **c** in β-$Ca_3(PO_4)_2$. Isolated spheres are Ca atoms,
457 interstitial in the eutactic monolayer of $[Ca(PO_4)_6]^{16-}$ ligands. Eutaxy is defined as having the

458 same geometric relationships as close-packing, without the requirement of being in contact
459 (O'Keeffe and Hyde 1996).

460 Figure 8b. A polyhedral layer in tuite viewed down **c**, which could reasonably be considered a
461 polymerized sheet of pinwheels.

462 Figure 9. The packing arrangement of tuite.

463 Figure 10a. The A' layer in tuite.

464 Figure 10b. The A layer in tuite

465

466

467

## List of Tables

Table 1. Summary of crystal data and refinement results for synthetic tuite.

| | | |
|---|---|---|
| Ideal chemical formula | $Ca_3(PO_4)_2$ | $Ca_3(PO_4)_2$ |
| Synthesis conditions | 15 GPa, 1300 °C | 12 GPa, 2300 °C |
| Starting material | $Ca_5(PO_4)_3Cl$ | $Ca_5(PO_4)_3OH$ |
| Crystal size (mm) | $0.05 \times 0.05 \times 0.04$ | $0.09 \times 0.09 \times 0.07$ |
| Space group | *R*-3*m* | *R*-3*m* |
| *a*(Å) | 5.2522(9) | 5.2487(6) |
| *c*(Å) | 18.690(3) | 18.674(3) |
| *V*(Å$^3$) | 446.5(2) | 445.5(1) |
| Z | 3 | 3 |
| $\rho_{cal}$(g/cm$^3$) | 3.461 | 3.469 |
| $\lambda$ (Å, Mo*K*α) | 0.71073 | 0.71069 |
| $\mu$ (mm$^{-1}$) | 3.33 | 3.20 |
| 2$\theta$ range for data collection | ≤66.08 | 60.0 |
| No. of reflections collected | 1495 | 753 |
| No. of independent reflections | 243 | |
| No. of reflections with $I > 2\sigma(I)$ | 216 | 201 [$I > 3\sigma(I)$] |
| No. of parameters refined | 19 | |
| R(int) | 0.016 | |
| Final $R_1$, $wR_2$ factors [$I > 2\sigma(I)$] | 0.018, 0.051 | 0.048, 0.053 |
| Final $R_1$, $wR_2$ factors (all data) | 0.021, 0.053 | |
| Goodness-of-fit | 1.080 | |
| | | |
| Reference | (1) | (2) |

References: (1) This study; (2) Sugiyama and Tokonami (1987).

Table 2. Coordinates and displacement parameters of atoms in synthetic tuite

| Atom | *x* | *y* | *z* | $U_{eq}$ | $U_{11}$ | $U_{22}$ | $U_{33}$ | $U_{23}$ | $U_{13}$ | $U_{12}$ |
|---|---|---|---|---|---|---|---|---|---|---|
| Ca1 | 0 | 0 | 0 | 0.0128(2) | 0.0163(3) | 0.0163(3) | 0.0058(3) | 0 | 0 | 0.0082(1) |
| Ca2 | 0 | 0 | 0.20359(2) | 0.0100(2) | 0.0116(2) | 0.0116(2) | 0.0069(2) | 0 | 0 | 0.0058(1) |
| P | 0 | 0 | 0.40508(3) | 0.0060(2) | 0.0064(2) | 0.0064(2) | 0.0052(3) | 0 | 0 | 0.0032(1) |
| O1 | 0 | 0 | 0.32372(8) | 0.0151(4) | 0.0193(6) | 0.0193(6) | 0.0066(7) | 0 | 0 | 0.0097(3) |
| O2 | 0.1737(1) | 0.3474(2) | 0.09950(4) | 0.0114(2) | 0.0139(4) | 0.0073(4) | 0.0106(4) | 0.0005(3) | 0.0002(1) | 0.0036(2) |

Table 3. Selected bond distances in synthetic tuite.

| | This study | Sugiyama and Tokonami (1987) |
|---|---|---|
| | Distance (Å) | Distance (Å) |
| Ca1-O1 x6 | 3.0377(5) | 3.0359(4) |
| -O2 x6 | 2.4404(9) | 2.440(3) |
| Ave. | 2.739 | 2.739 |
| Ca2-O1 | 2.245(2) | 2.239(5) |
| -O2 x3 | 2.507(1) | 2.509(4) |
| -O2 x6 | 2.6870(5) | 2.686(2) |
| Ave. | 2.589 | 2.588 |
| P--O1 | 1.521(2) | 1.526(6) |
| --O2 x3 | 1.542(1) | 1.535(2) |
| Ave. | 1.537 | 1.533 |

530 Table 4. Crystallographic parameters for $CaSiO_3$ and $Ca_3(PO_4)_2$ system minerals. $U_{cp}$ is a measure of the distortion of the packing
531 arrangement from perfect closest-packing (Thompson and Downs 2001). A value of zero is perfectly closest-packed, and distortion
532 increases as values of $U_{cp}$ get larger.

| Name | Chemistry | Stacking | Ca Packing? | ρ (gm/cm$^3$) | $U_{cp}$ (Å$^2$) | Reference |
|---|---|---|---|---|---|---|
| pseudowollastonite | $CaSiO_3$ | ABABACAC | Y | 2.90 | - | Yang and Prewitt 1999 |
| wollastonite | $CaSiO_3$ | - | - | 2.95 | - | Ohashi and Finger 1978 |
| high-pressure phase | $Ca_{.96}Fe_{.04}SiO_3$ | CCP (ABC) | N | 3.05 | 2.6 | Trojer 1969 |
| Ca-perovskite | $CaSiO_3$ | CCP (ABC) | Y | 4.33 | 0 | Caracas and Wentzcovitch 2006 |
| α-$Ca_3(PO_4)_2$ | $Ca_3(PO_4)_2$ | - | - | 2.81 | - | Mathew et al. 1977 |
| β-$Ca_3(PO_4)_2$ | $Ca_3(PO_4)_2$ | CCP (ABC) | N | 3.07 | 24.7 | Dickens et al. 1974 |
| γ-$Ca_3(PO_4)_2$ tuite | $Ca_3(PO_4)_2$ | - | - | 3.46 | - | this work |

533

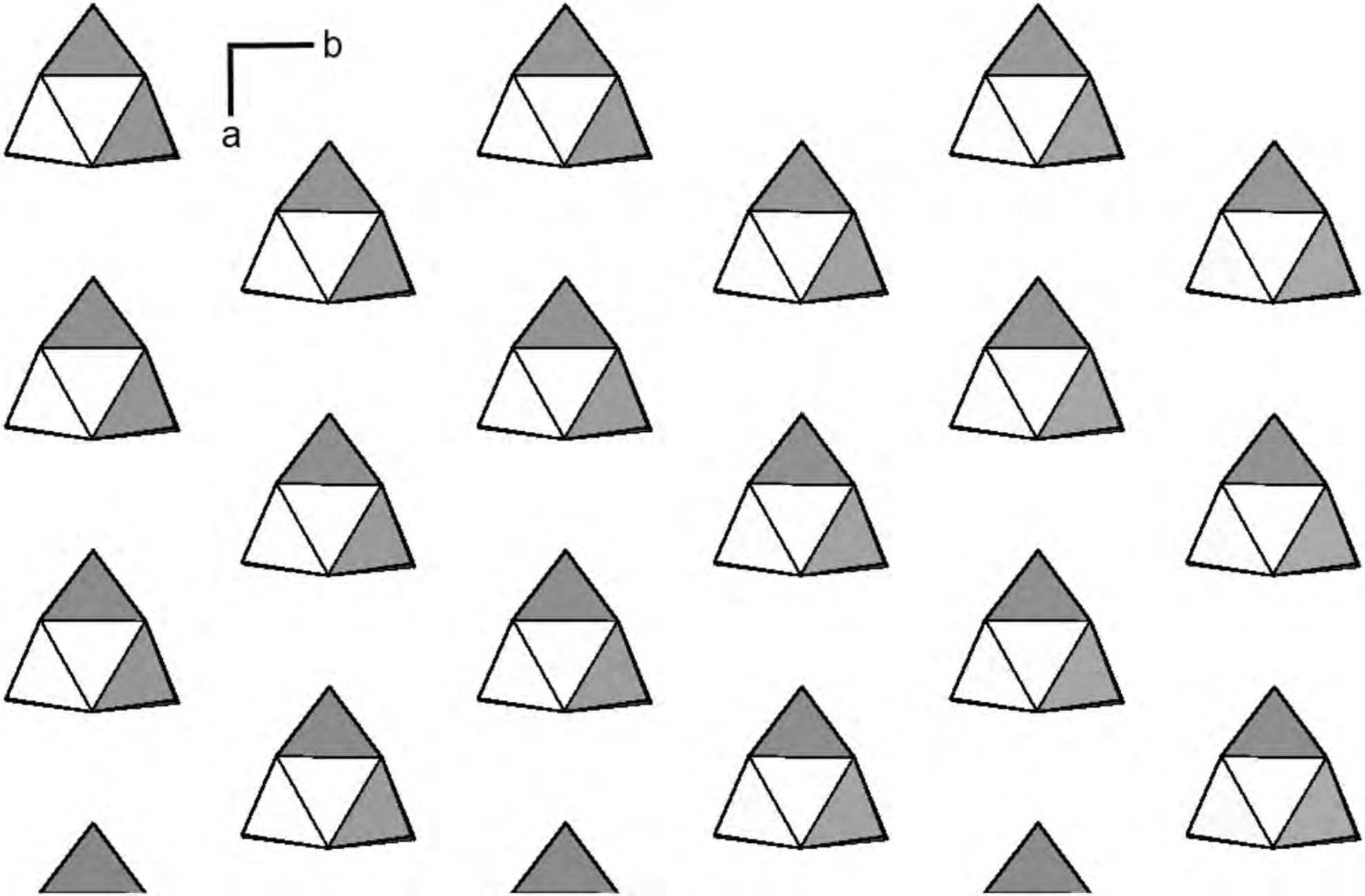


Figure 1a

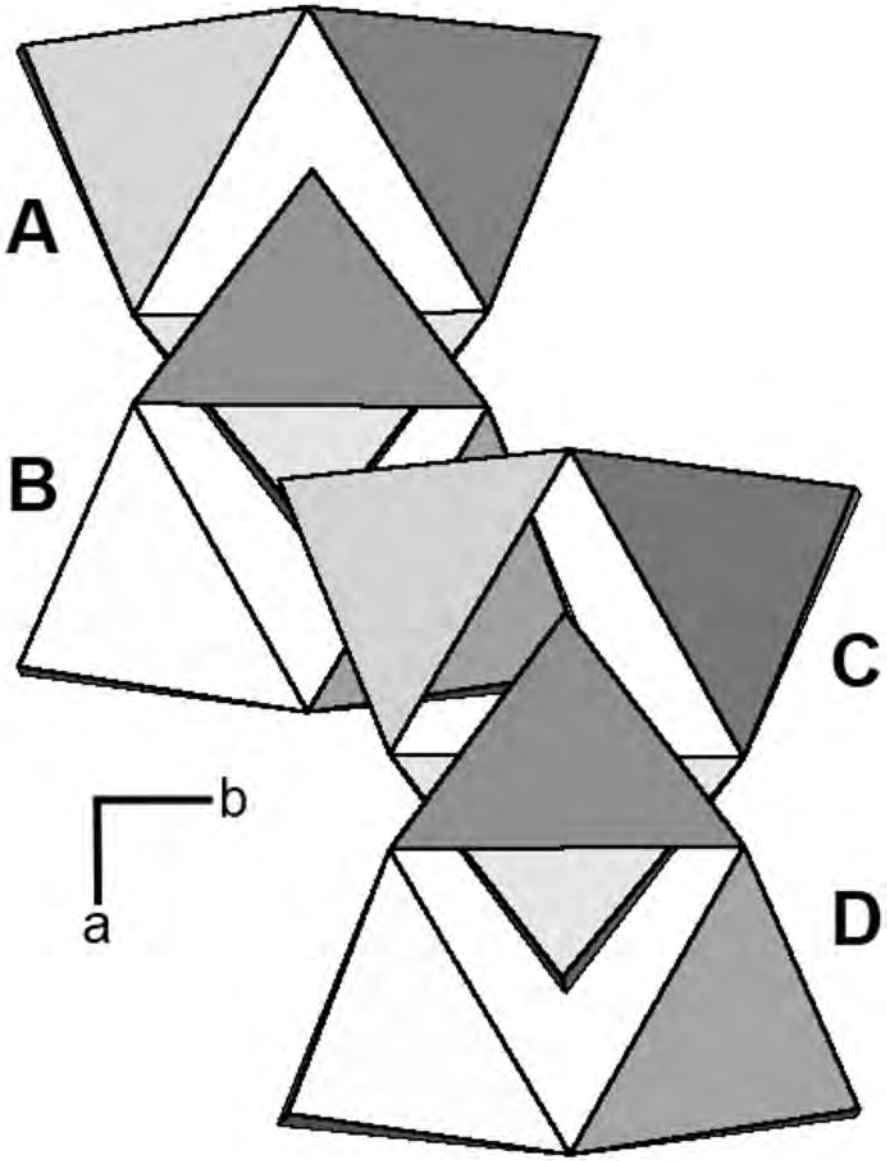


Figure 1b

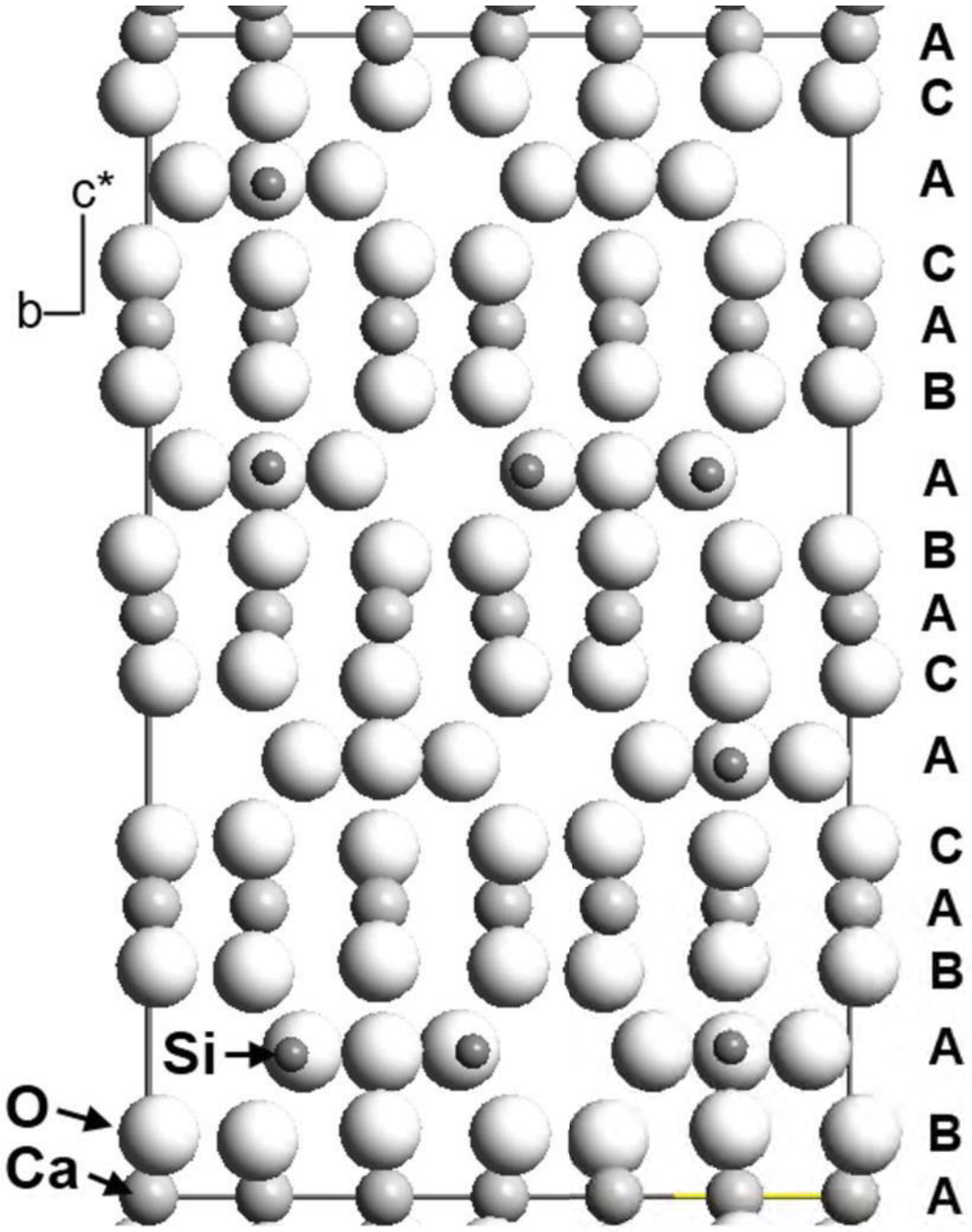


Figure 2

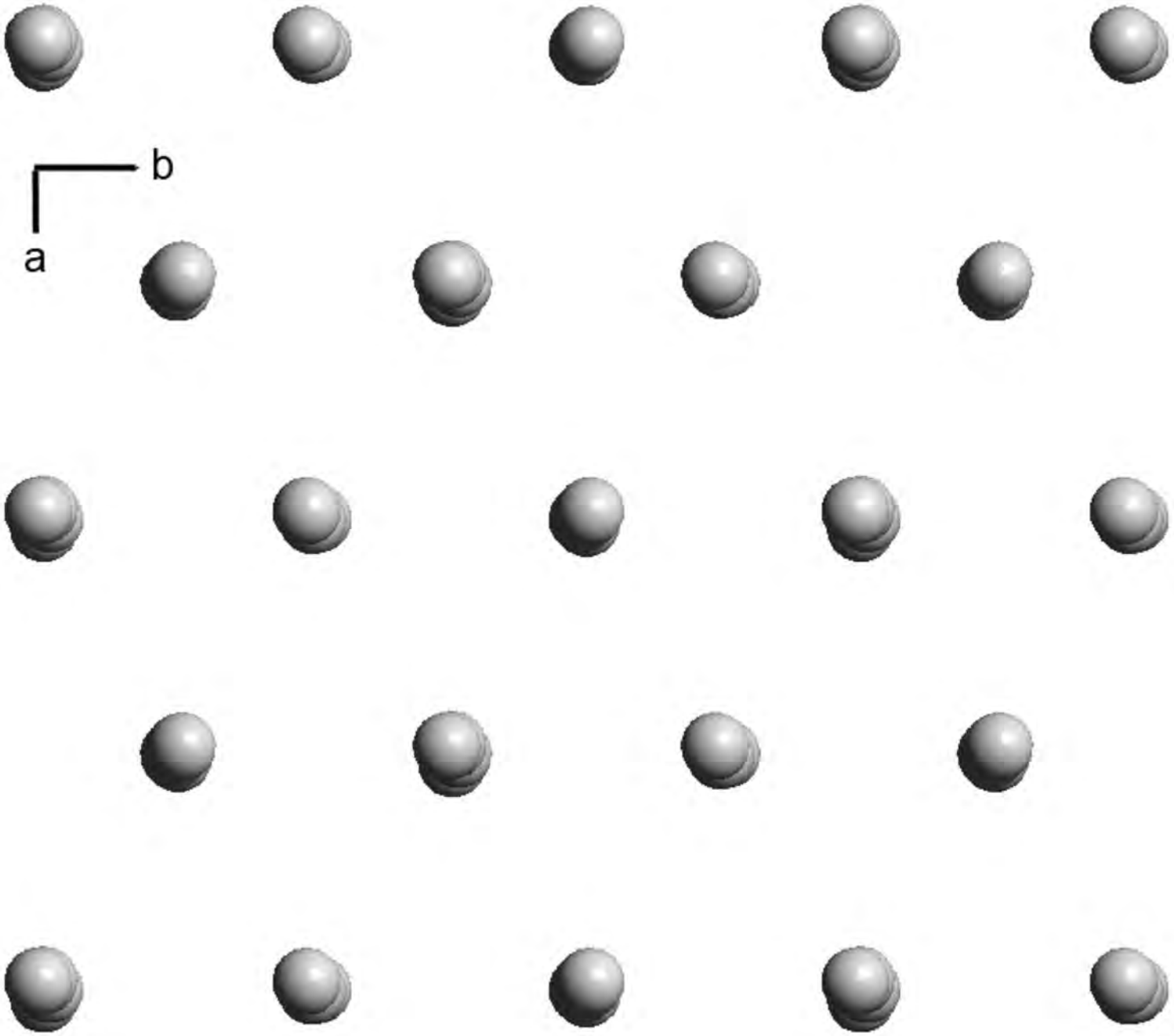


Figure 3

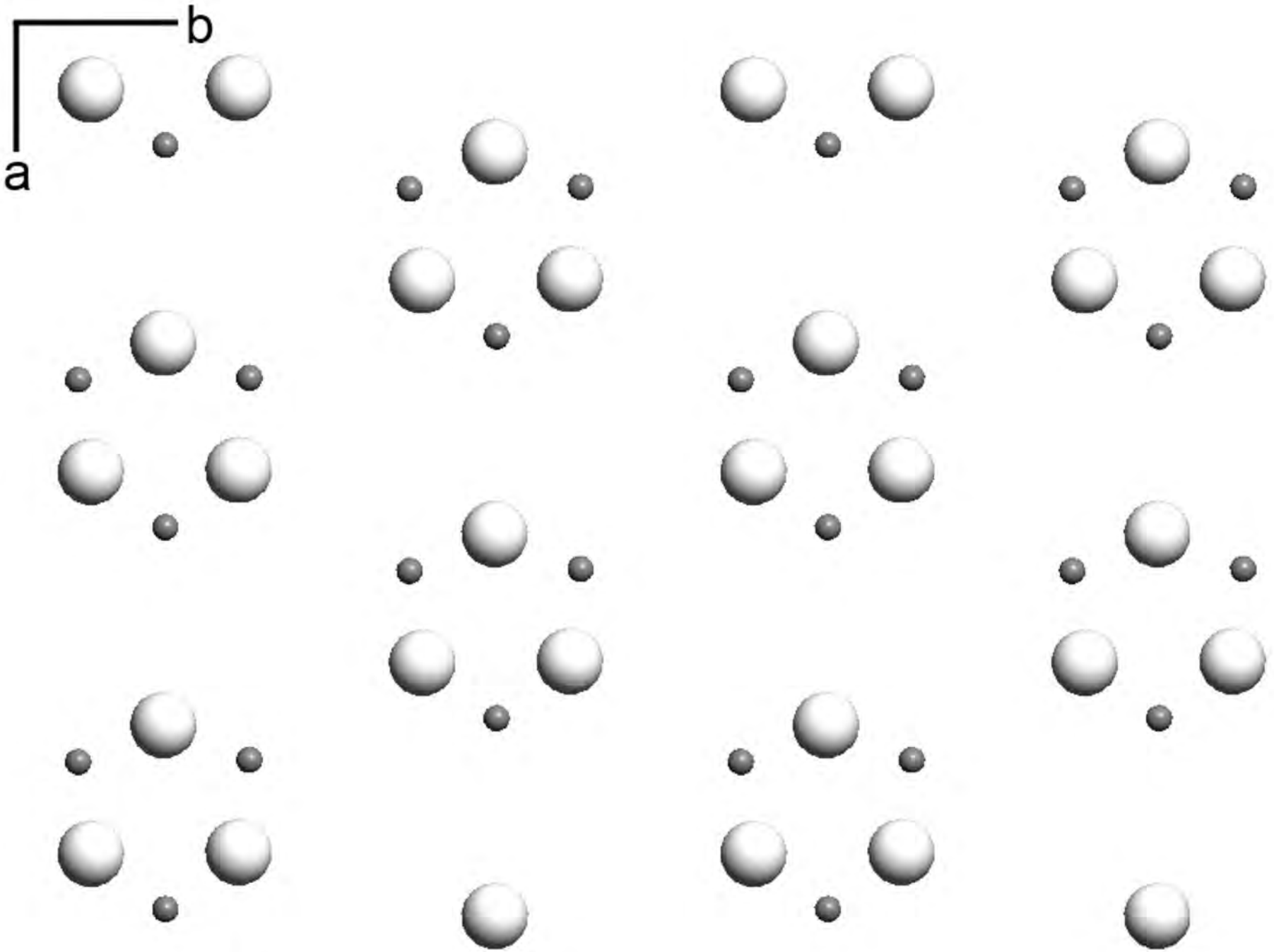


Figure 4a

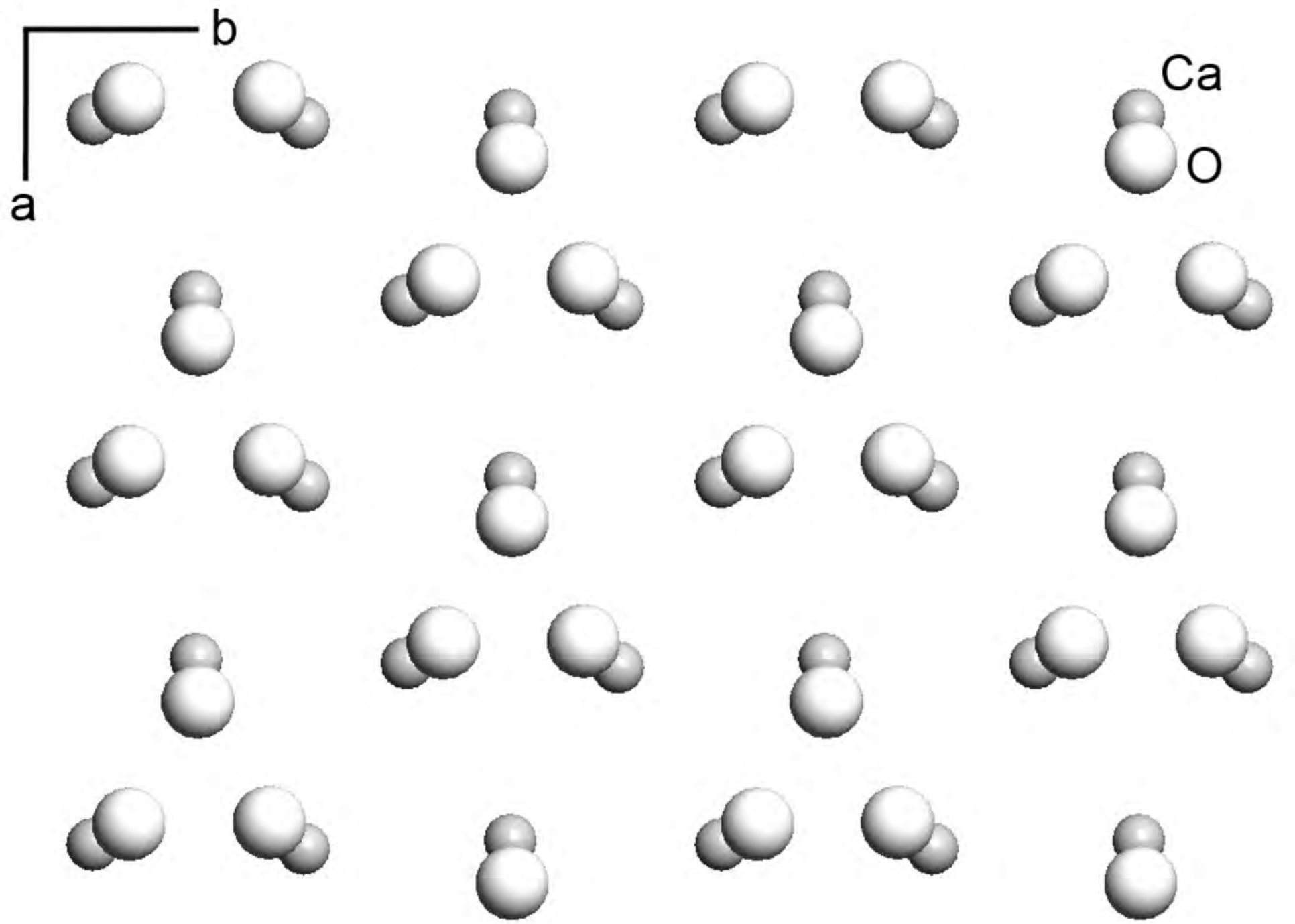


Figure 4b

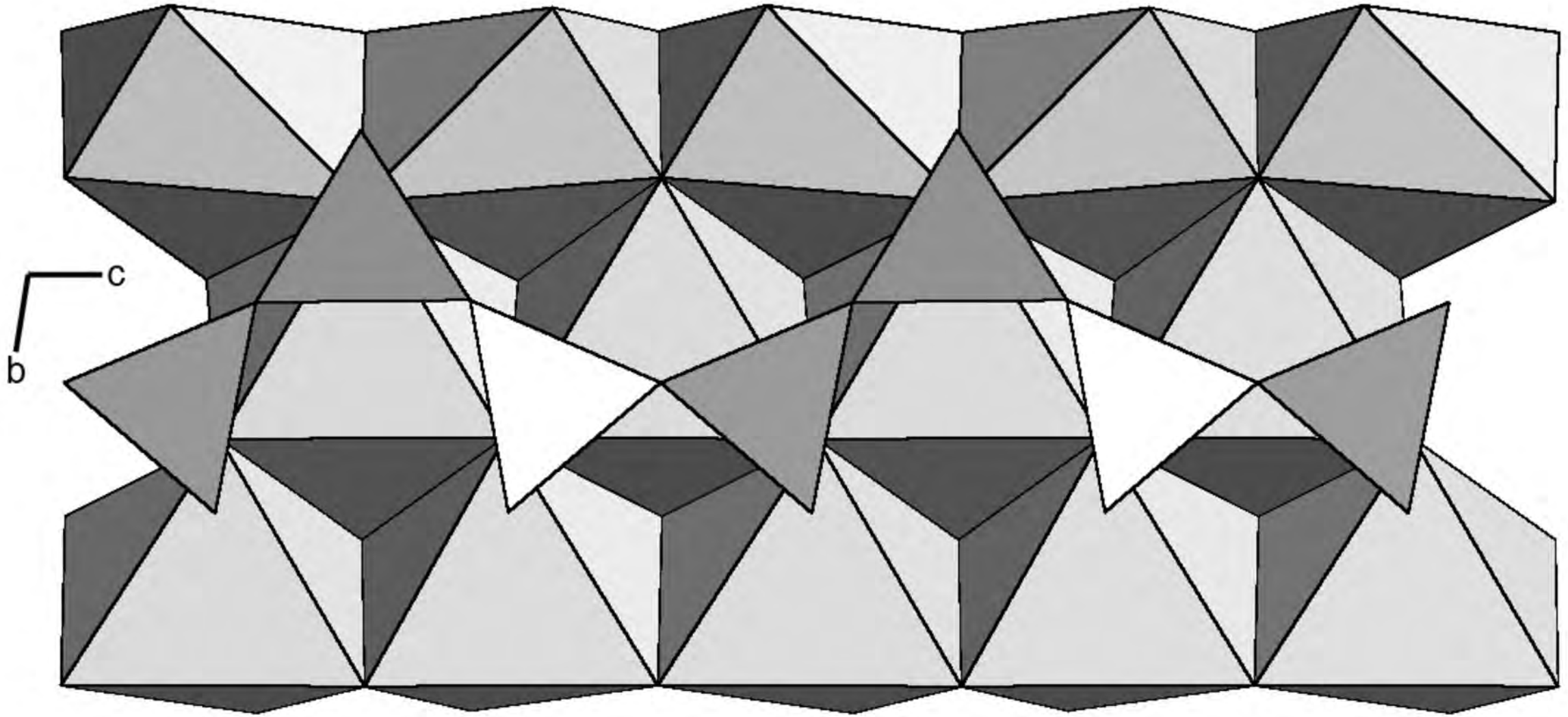


Figure 5a

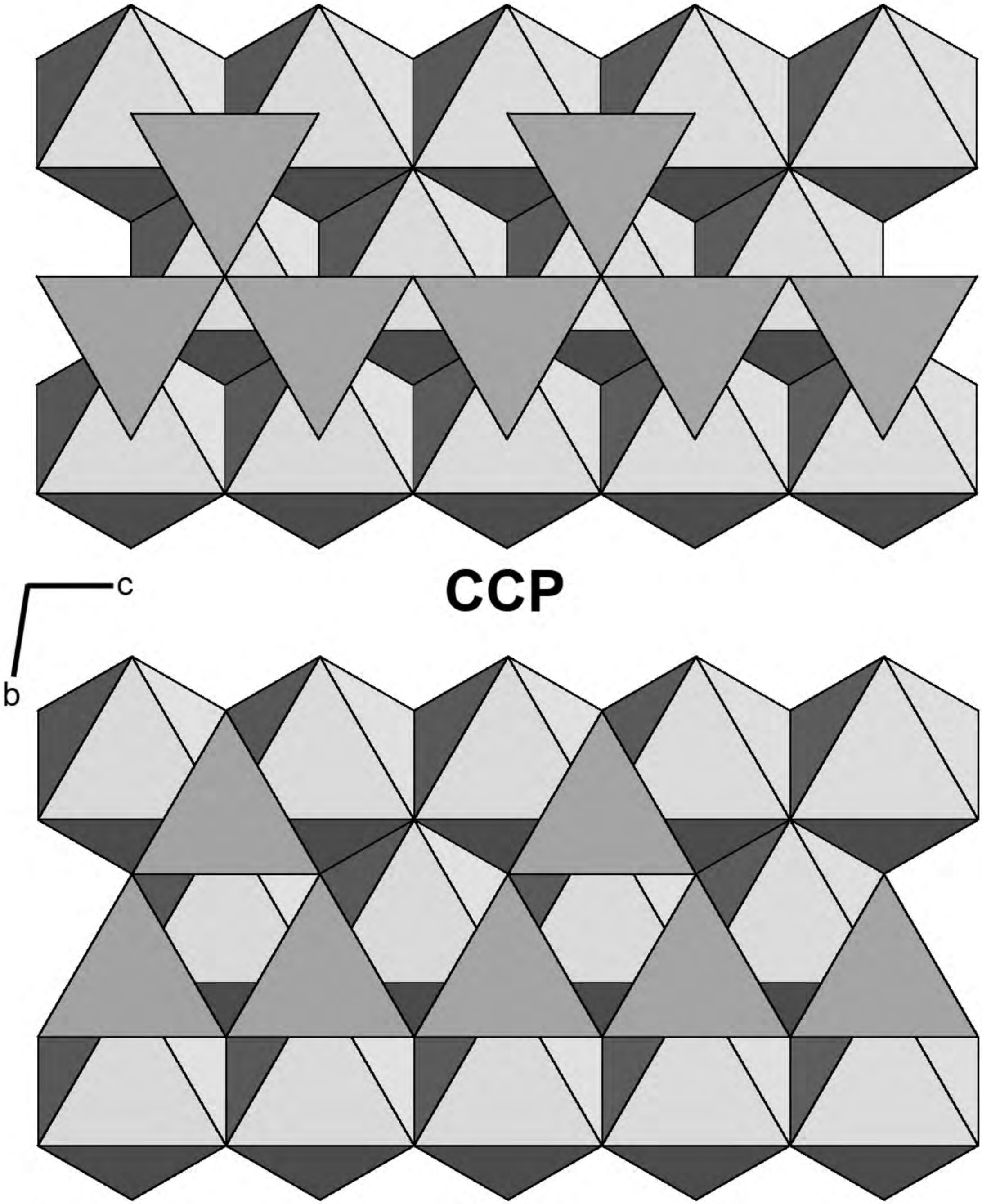


Figure 5b

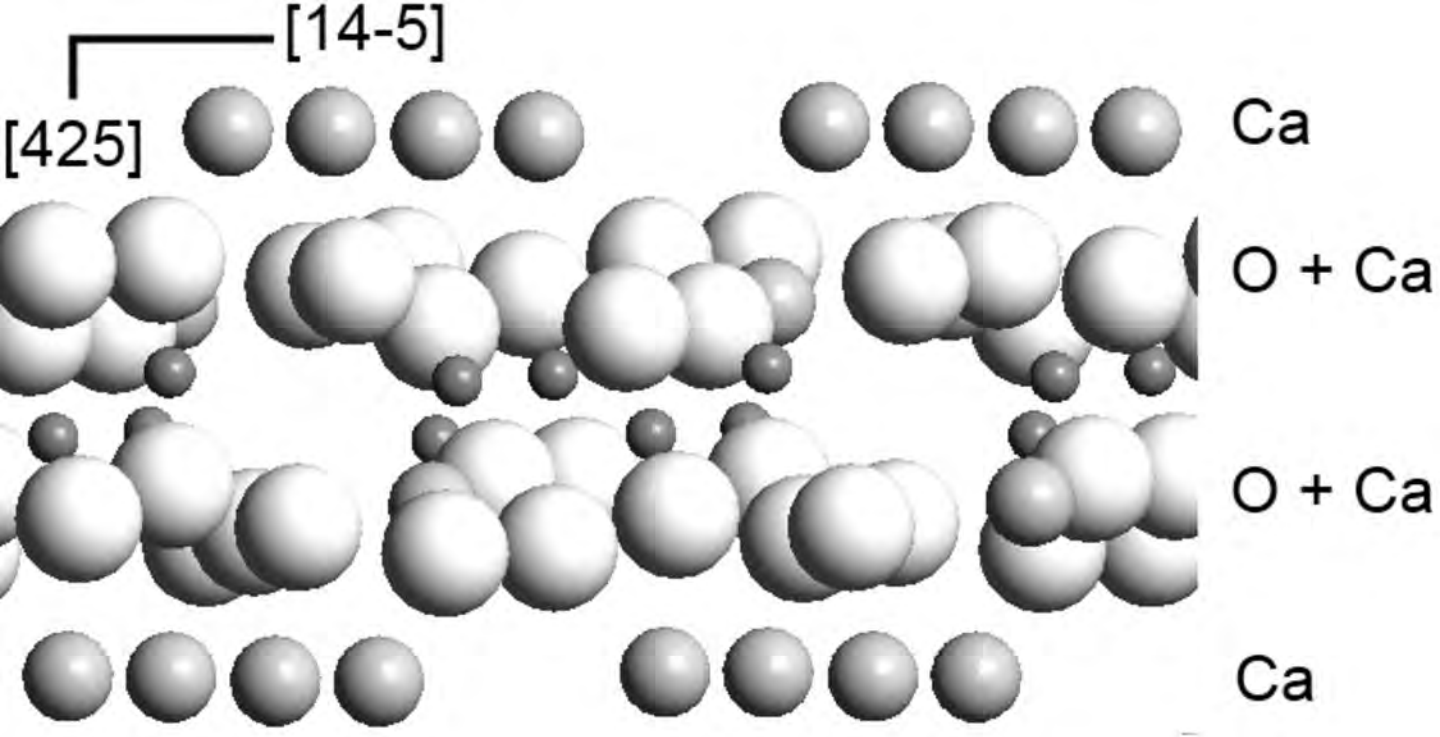


Figure 6a

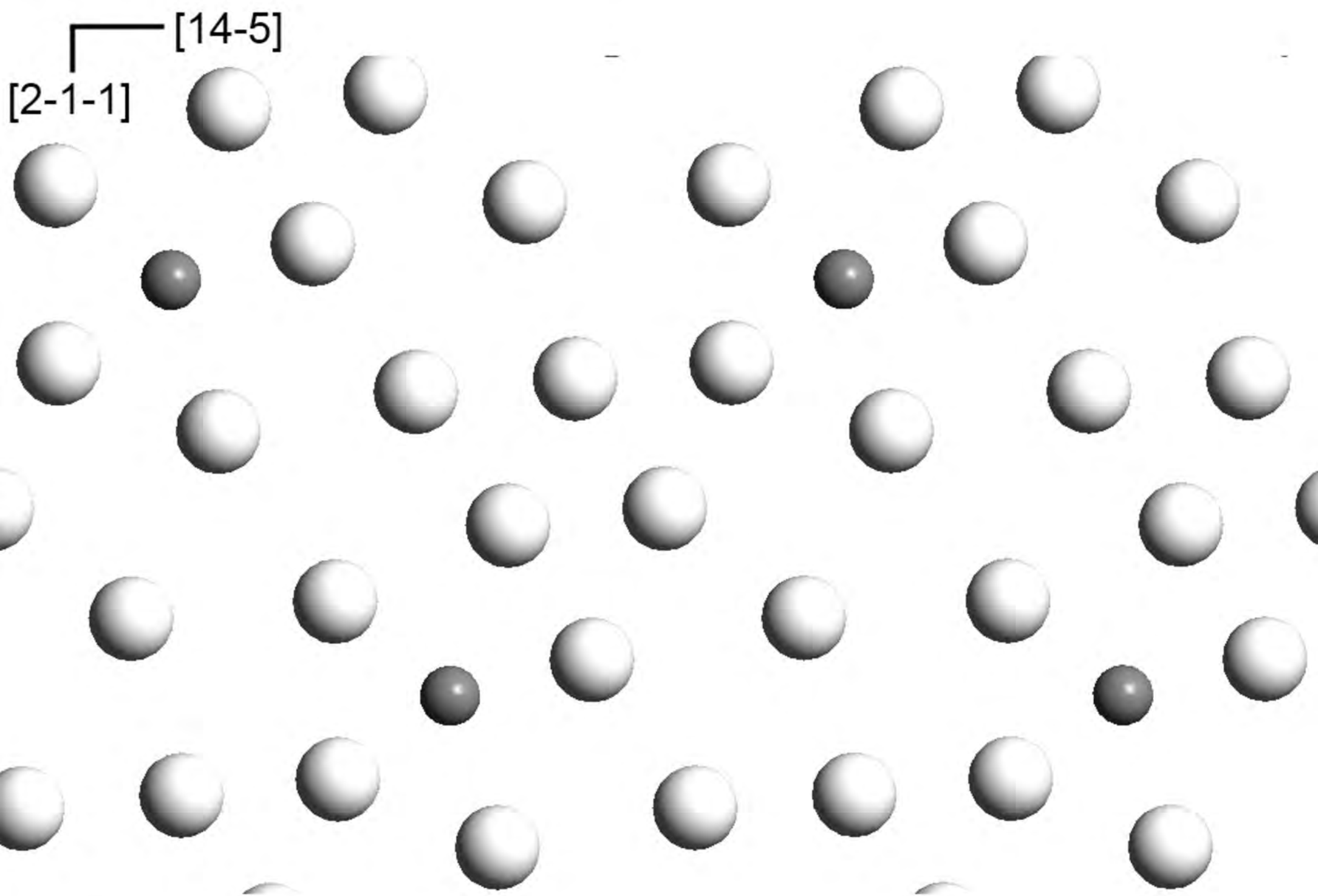


Figure 6b

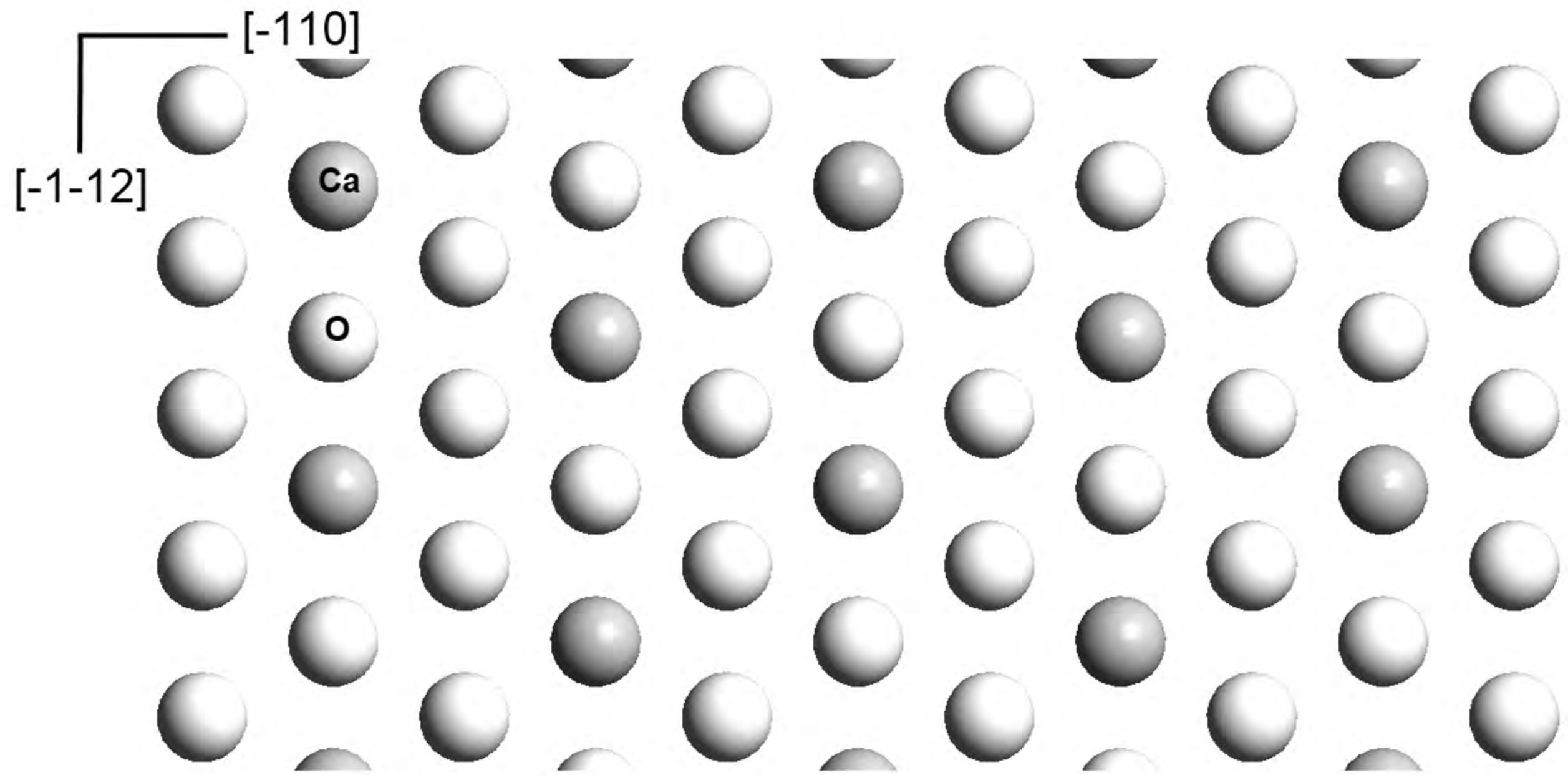


Figure 7

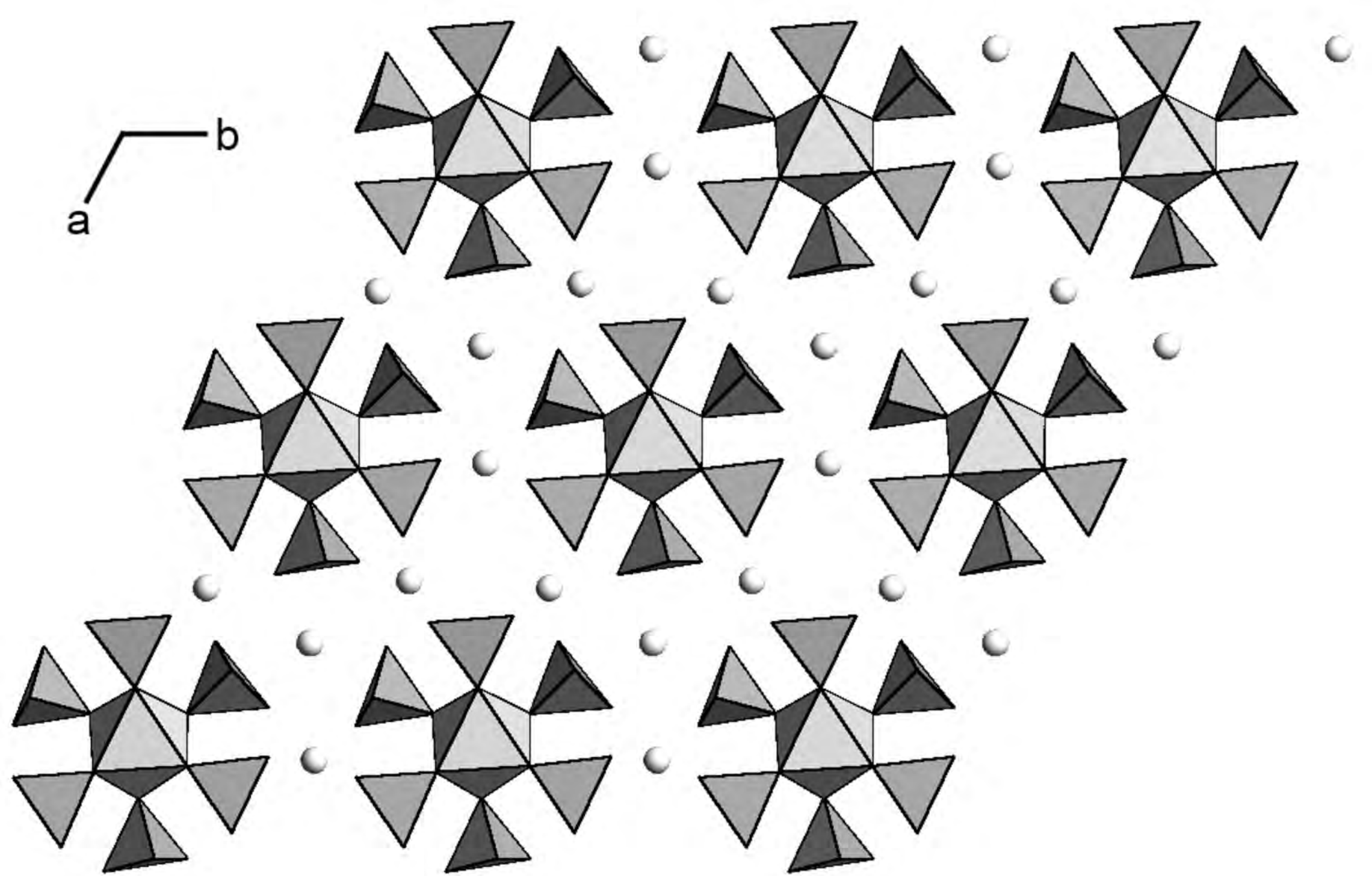


Figure 8a

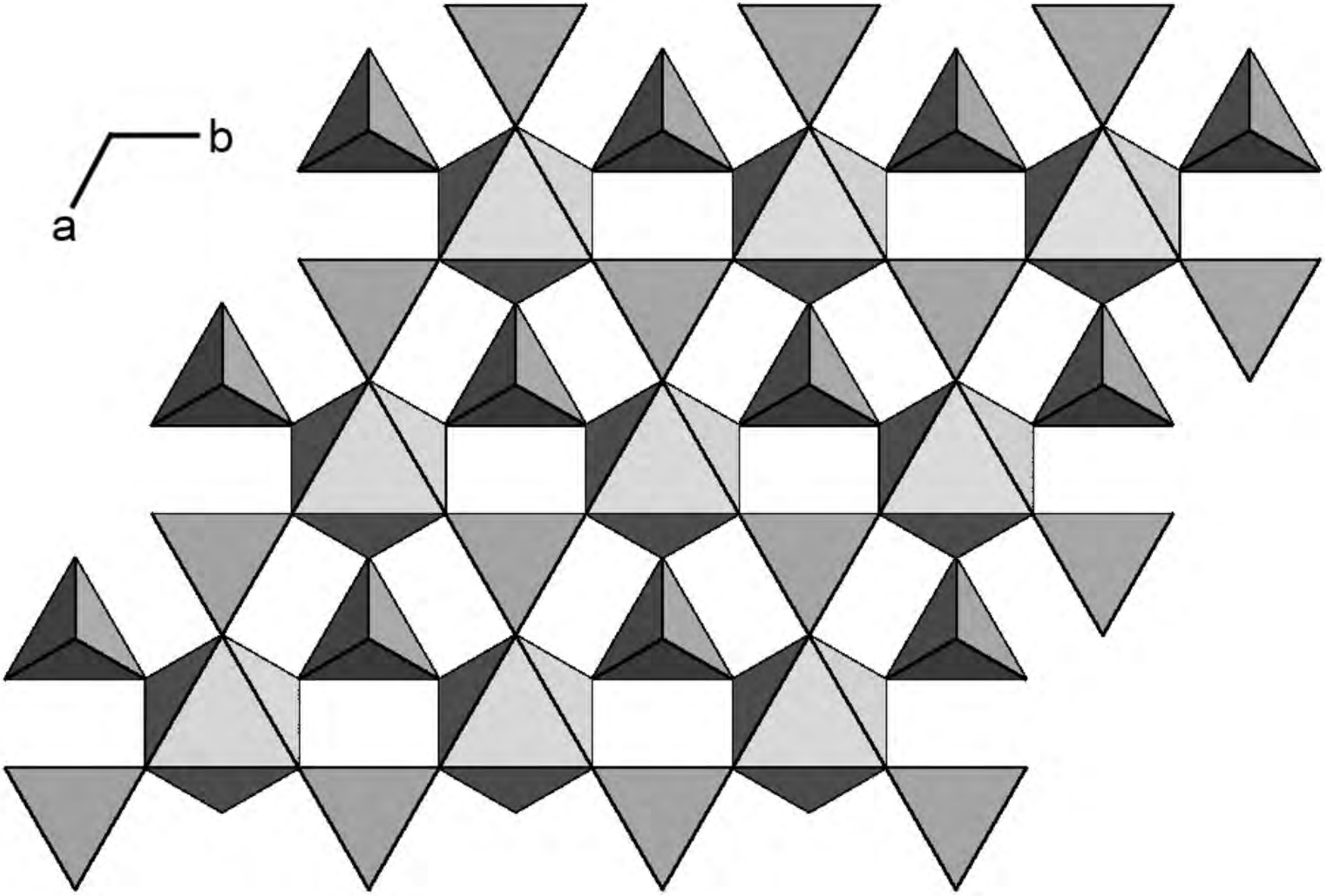


Figure 8b

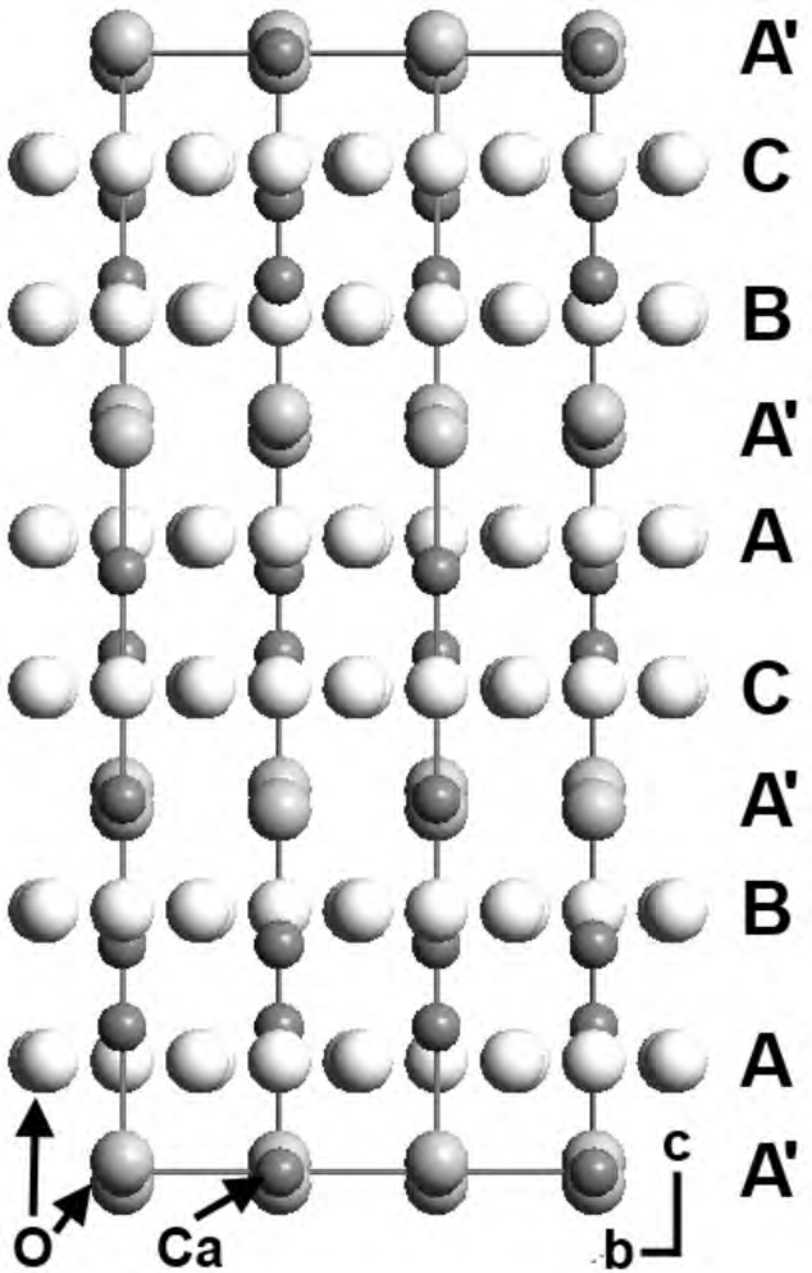


Figure 9

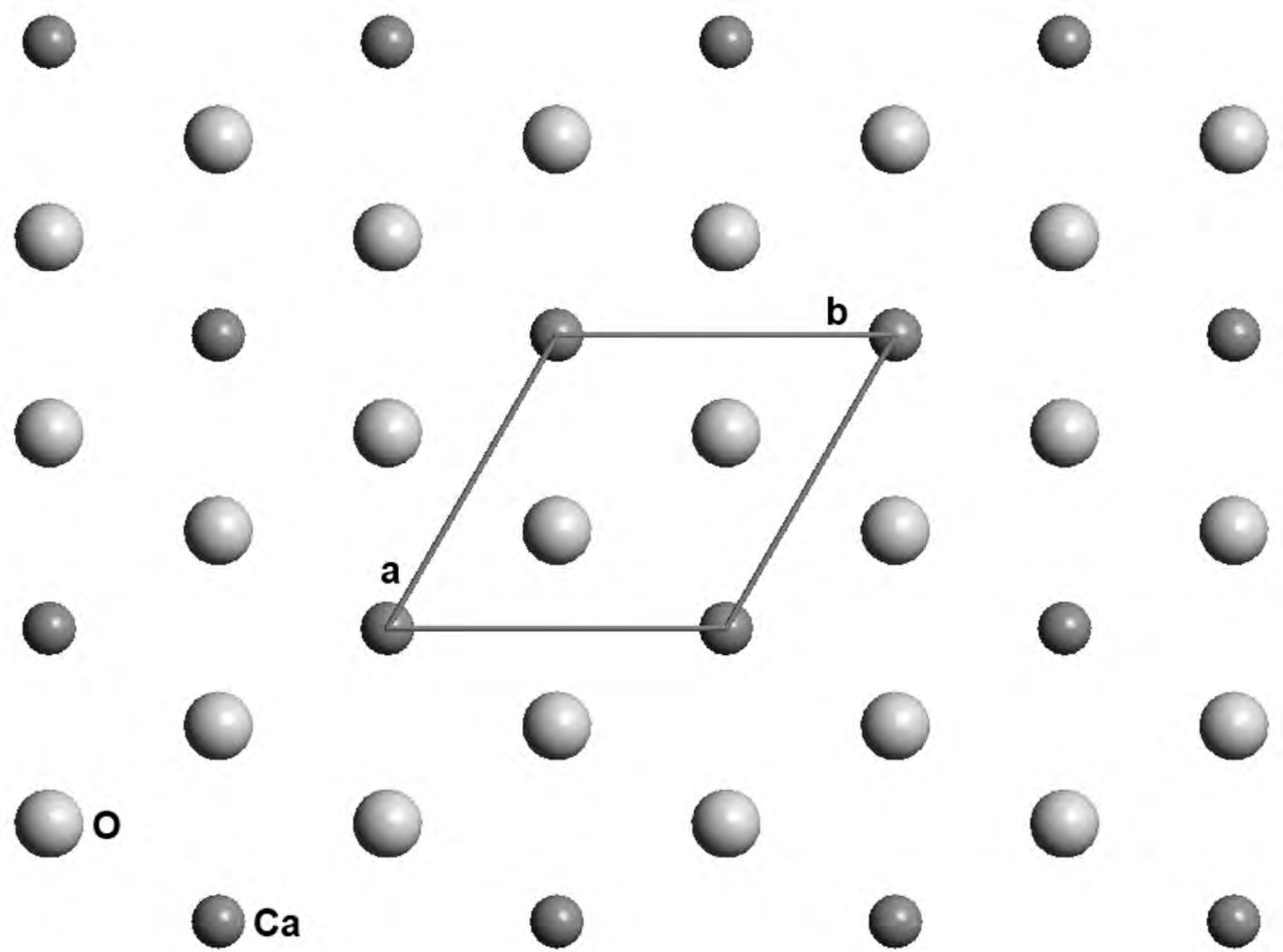


Figure 10a

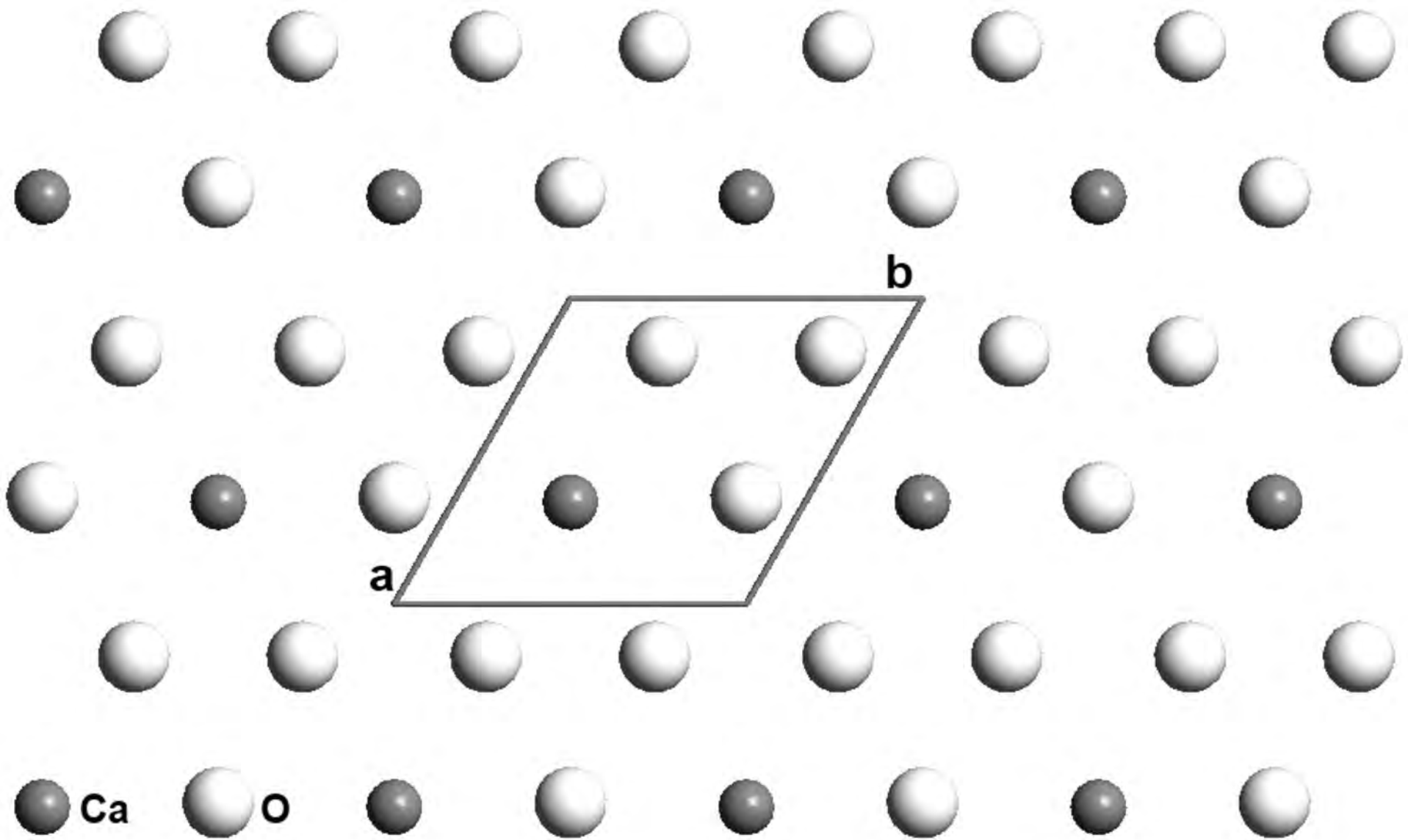


Figure 10b